







# Measuring the Hubble Constant with GW190521 as an Eccentric black hole Merger and Its Potential Electromagnetic Counterpart

V. Gayathri<sup>1</sup>, J. Healy<sup>2</sup>, J. Lange<sup>2</sup>, B. O’Brien<sup>1</sup>, M. Szczepanczyk<sup>1</sup>, I. Bartos<sup>1</sup> , M. Campanelli<sup>2</sup> , S. Klimenko<sup>1</sup>,  
C. O. Lousto<sup>2</sup> , and R. O’Shaughnessy<sup>2</sup> 

<sup>1</sup> Department of Physics, University of Florida, PO Box 118440, Gainesville, FL 32611-8440, USA; [imrebartos@ufl.edu](mailto:imrebartos@ufl.edu)

<sup>2</sup> Center for Computational Relativity and Gravitation, Rochester Institute of Technology, Rochester, NY 14623, USA; [rossma@rit.edu](mailto:rossma@rit.edu)

Received 2020 September 29; revised 2021 February 3; accepted 2021 February 5; published 2021 February 22

## Abstract

Gravitational-wave observations can be used to accurately measure the Hubble constant  $H_0$  and could help understand the present discrepancy between constraints from Type Ia supernovae and the cosmic microwave background. Neutron star mergers are primarily used for this purpose as their electromagnetic emission can be used to greatly reduce measurement uncertainties. Here we quantify the implied  $H_0$  using the recently observed black hole merger GW190521 and its candidate electromagnetic counterpart found by ZTF using a highly eccentric explanation of the properties of GW190521. As the electromagnetic association is currently uncertain, our main goal here is to determine the effect of eccentricity on the estimated  $H_0$ . We obtain  $H_0 = 68.8_{-25.5}^{+45.7}$  km s<sup>-1</sup> Mpc<sup>-1</sup>. Our results indicate that future  $H_0$  computations using black hole mergers will need to account for possible eccentricity. For extreme cases, the orbital velocity of binaries in active galactic nucleus disks can represent a significant systematic uncertainty.

*Unified Astronomy Thesaurus concepts:* Gravitational wave astronomy (675); Cosmology (343)

## 1. Introduction

With a total mass of around  $150 M_\odot$ , the binary black hole merger GW190521 was the heaviest system detected to date through gravitational waves by LIGO and Virgo (Aasi et al. 2015; Acernese et al. 2015; Abbott et al. 2020a). The heavier black hole in the binary had a mass of about  $85 M_\odot$ . Such a mass is typically not expected from stellar evolution due to pair instability that prevents some of the most massive stars from leaving a compact remnant (Woosley et al. 2007; Abbott et al. 2020b). In addition, the black holes’ spins are found to be large and misaligned with the binary orbit, disfavoring the possibility that the system is originated from a stellar binary (Abbott et al. 2020b). Nevertheless, uncertainties in stellar evolution remain, and some recent results indicate that low-metallicity stars may produce black hole masses within the mass gap (Belczynski 2020; Farrell et al. 2020).

A possible explanation for the observed properties of GW190521 is that it is a so-called hierarchical merger—the black holes in the binary are themselves the remnants of past black hole mergers (Miller & Hamilton 2002; O’Leary et al. 2006; Giersz et al. 2015). This scenario can naturally lead to masses in excess to the  $\sim 65 M_\odot$  pair-instability limit. It also results in higher black hole spins, consistent with the high reconstructed spins of  $0.69_{-0.62}^{+0.27}$  and  $0.73_{-0.64}^{+0.24}$  for the two black holes in GW190521 (Abbott et al. 2020a). In addition, the hierarchical merger scenario implies that black holes form a binary after a chance encounter, in which their spin will be randomly oriented. This is consistent with the reconstructed misalignment between the binary orbit and black hole spins in GW190521 (Abbott et al. 2020a).

By comparing the observed gravitational waveform to numerical relativity simulations, Gayathri et al. (2020b) found that GW190521 could be a highly eccentric merger (hereafter UF/RIT model). This result further supports the binary’s origin as a dynamical encounter within a dense black hole population. Binaries lose any existing eccentricity over time due to

gravitational radiation, therefore only binaries that formed soon before merger can retain any eccentricity. Such formation is possible in chance encounters but not in systems originating in isolated stellar binaries.

Active galactic nuclei (AGNs) represent a well-suited environment to produce hierarchical black hole mergers (Bartos et al. 2017b, 2017a; Stone et al. 2017; McKernan et al. 2018; Yang et al. 2019b, 2019a; Tagawa et al. 2020b, 2020a; Yang et al. 2020). Galactic nuclei harbor a dense population of black holes (O’Leary et al. 2009; Hailey et al. 2018) that are further compressed through interaction with the AGN disk. Dynamical friction can align the orbits of some of the black holes with the disk plane, where they migrate inward and can merge with each other. As merger remnants can remain within the disk, consecutive mergers are common and could represent the majority of AGN-assisted events. Several binaries discovered by LIGO/Virgo have properties suggestive of their possible AGN origin (Yang et al. 2019b; Gayathri et al. 2020a; Yang et al. 2020a; Tagawa et al. 2020a). Other astrophysical sites can also produce hierarchical mergers, including star clusters (Fragione et al. 2020). A heavy black hole merger such as GW190521 could also have been produced by the merger of ultra-dwarf galaxies (Palmese & Conselice 2020).

Following the public alert issued by LIGO/Virgo on the detection of GW190521 (LIGO & Virgo 2019), the Zwicky Transient Facility (ZTF) carried out a search for excess optical emission from an AGN within the publicly available localization volume of GW190521. It identified a possible counterpart that was interpreted as being due to the accreting black hole remnant of the GW190521 merger (Graham et al. 2020). As this is the first such observation and since there are open questions about the emission processes involved, more studies and probably further similar detections are needed to confidently establish the connection between the transient and GW190521. However, for the purposes of understanding the consequences of such a connection, in the following we assume

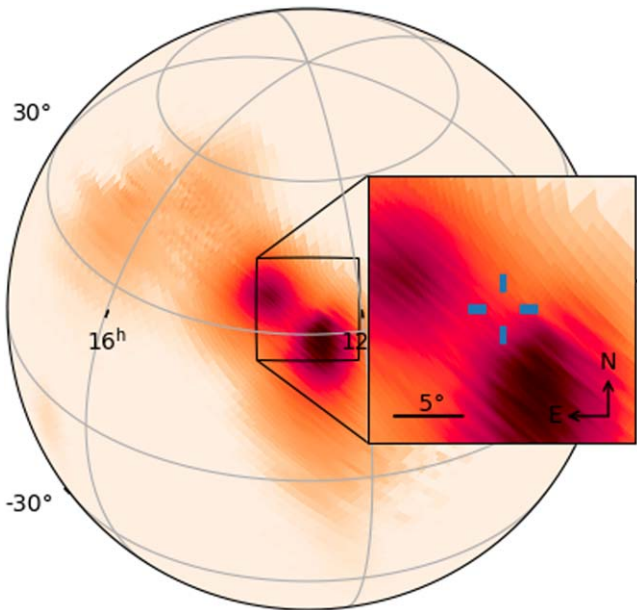


**Figure 1.** Sky location reconstructed for GW190521 using the UF/RIT model with  $e \sim 0.7$  (Gayathri et al. 2020b). In the inset panel, the reticle marks the position of the apparent host AGN candidate J124942.3+344929 (Graham et al. 2020).

that the electromagnetic emission is indeed produced by the merger remnant.

If GW190521 indeed produced an observed electromagnetic counterpart, it could contribute to the measurement of cosmological parameters (Schutz 1986; Abbott et al. 2017, 2019; Soares-Santos et al. 2019).

In this Letter we constrain  $H_0$  using GW190521 and its candidate ZTF counterpart. We use the reconstructed properties of GW190521 by the UF/RIT model in which the event was a highly eccentric black hole binary with eccentricity  $e \sim 0.7$  (Gayathri et al. 2020b).

The Letter is organized as follows. We describe our computation of  $H_0$  in Section 3. We present our localization results and the computed  $H_0$  for GW190521 in Sections 2 and 4, respectively. We conclude in Section 5.

## 2. Source Localization

Due to its large distance and high mass, GW190521 has one of the largest localization volumes among LIGO/Virgo events so far. This increases the chance of a chance electromagnetic association compared to other black hole mergers. Using the UF/RIT model with eccentricity  $e \sim 0.7$  (Gayathri et al. 2020b) we obtain a localization sky area of  $100 \text{ deg}^2$  ( $500 \text{ deg}^2$ ) at 50% (90%) confidence level (see Figure 1), and a localization volume of  $0.16 \text{ Gpc}^3$  ( $1.24 \text{ Gpc}^3$ ) at 50% (90%) confidence level. In addition, the ZTF candidate counterpart associated with AGN J124942.3+344929 (Graham et al. 2020) at the 97% credible level of the GW190521 localization volume, and ZTF only searched for a counterpart in its observable sky area and among cataloged AGNs. Therefore, further evidence will be needed for confident association (Ashton et al. 2020). Nonetheless, in the following we will consider the consequences of such possible association.

We used the recorded gravitational-wave data  $\mathcal{D}_{\text{GW}}$  to compute the probability density  $p(d_L|\mathcal{D}_{\text{GW}})$  of the merger’s luminosity distance  $d_L$ . We used the RIFT parameter estimation

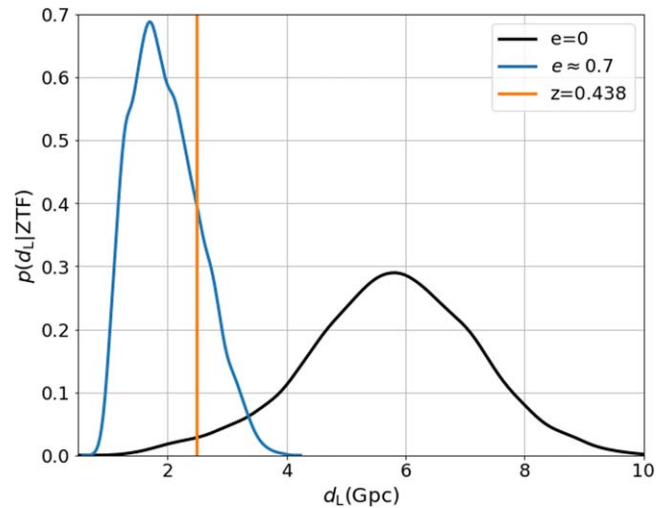


**Figure 2.** Luminosity distance probability distribution obtained using NRSur7dq4 gravitational waveforms (Varma et al. 2019) assuming eccentricity  $e = 0$  (red), and using the UF/RIT model with eccentricity  $e \sim 0.7$  (Gayathri et al. 2020b) (black). These distributions are obtained using RIFT algorithm for fixed source direction to that of the ZTF source. The vertical line shows the distance of the ZTF source assuming Planck 2018 cosmology (Aghanim et al. 2018).

package (Abbott et al. 2016; Healy et al. 2018; Lange et al. 2018, 2017) to obtain this probability density. We fixed the source direction to that of the ZTF candidate,  $\Omega_{\text{ZTF}}$ . We carried out this computation for both the UF/RIT model with  $e \sim 0.7$  obtained using numerical relativity simulations (Gayathri et al. 2020b), and for a noneccentric model derived using NRSur7dq4 waveforms (Varma et al. 2019). For both models we assumed that the electromagnetic counterpart is always detectable from this source type independently from the source direction and distance. We adopted a uniform volumetric source probability density, which is a good approximation of the expected distribution of AGN-assisted mergers (Yang et al. 2020). We further adopted a uniform prior on the cosine of the binary’s inclination. For the  $e \sim 0.7$  model we adopted mass and spin parameters from the maximum-likelihood waveform (Gayathri et al. 2020b). For the  $e = 0$  model we used uniform probability densities for the black hole masses within  $[30M_\odot, 200M_\odot]$ , uniform spin amplitudes, and isotropic spin orientations.

In Figure 2 we show  $p(d_L|\mathcal{D}_{\text{GW}}, \Omega_{\text{ZTF}})$  for the UF/RIT model with  $e \sim 0.7$  (Gayathri et al. 2020b) and also one derived using the NRSur7dq4 waveform model (Varma et al. 2019) assuming  $e = 0$ . While Abbott et al. (2020a) reconstruct a distance of  $d(\text{NRSur7dq4}) = 5.3^{+1.5}_{-1.5}$  Gpc, Gayathri et al. (2020b) obtain  $d(e \sim 0.7) = 1.8^{+1.1}_{-0.1}$  Gpc. The two distributions are markedly different for these two cases (see also Calderón Bustillo et al. 2020). The distance distribution for  $e = 0$  is somewhat dependent on the choice of distance prior and the used gravitational waveform family, as can be seen by comparing our result to those of Mukherjee et al. (2020), see their Figure 1) and Chen et al. (2020, see their Figure 1).

The ZTF candidate counterpart was associated with AGN J124942.3+344929 with measured redshift  $z_{\text{ZTF}} = 0.438$  (Graham et al. 2020). In Figure 2 we also show the distance  $d_{\text{ZTF}} \approx 2.5 \text{ Gpc}$  of the ZTF candidate assuming Planck 2018 cosmology (Aghanim et al. 2018). We see that both  $e \sim 0.7$  and  $e = 0$  models are consistent with this distance, with somewhat higher probability density for the eccentric case.

While Abbott et al. (2020a) reconstruct a distance of  $d(\text{NRSur7dq4}) = 5.3_{-1.5}^{+1.5}$  Gpc, Gayathri et al. (2020b) obtain  $d(e \sim 0.7) = 1.8_{-0.1}^{+1.1}$  Gpc.

### 3. Computing the Hubble Constant

The Hubble constant  $H_0$  describes the local expansion rate of the universe. It is expressed as  $v_h = H_0 d_L$ , where  $v_h$  is Hubble flow velocity and  $d_L$  is the luminosity distance to the source.

Gravitational waves from compact binary mergers enable us to directly measure the luminosity distance of the source. If we are able to identify a binary's host galaxy, the host galaxy provides information on the binary's redshift. As gravitational-wave localization is typically limited, the host galaxy identification relies primarily on the detection of electromagnetic emission from the binary. Once we have an estimated redshift for the source, for fixed  $d_L$  one can estimate the Hubble constant (Hogg 1999) using

$$H_0(d_L, z) = \frac{c(1+z)}{d_L} \int_0^z \frac{dz'}{E(z')} \quad (1)$$

with

$$E(z) = \sqrt{\Omega_r(1+z)^4 + \Omega_m(1+z)^3 + \Omega_k(1+z)^2 + \Omega_\Lambda}. \quad (2)$$

Here,  $c$  is the speed of light,  $\Omega_r$  is the radiation energy density,  $\Omega_m$  is matter density,  $\Omega_\Lambda$  is the dark energy density, and  $\Omega_k$  is the curvature of our universe. We adopted a set of cosmology parameters  $\{\Omega_r, \Omega_m, \Omega_k, \Omega_\Lambda\} = \{0, 0.306, 0, 0.694\}$  measured by the Planck Collaboration (Aghanim et al. 2018). We considered these parameters fixed when recovering  $H_0$  as their uncertainties are much smaller than other uncertainties here. Here we have considered uniform prior on  $H_0$ . Given the Gpc distance scale of the event, we neglected the peculiar velocity of the host galaxy.

We also neglected any motion of the binary within the galaxy. Since binary mergers in AGNs occur very close to the central supermassive black hole, their orbital velocities can be substantial. This can distort the gravitational waveform, biasing our cosmological measurement. Considering the mass of the supermassive black hole in the candidate AGN,  $M_{\text{SMBH}} = 10^8 - 10^9 M_\odot$  (Graham et al. 2020), and the characteristic distance  $10^{-2}$  pc of the merger from the supermassive black hole, the rotational velocity of the binary is  $10^4 \text{ km s}^{-1}$ . At the reconstructed distance of GW190521, this velocity corresponds to a 1%–30% error on the reconstructed Hubble constant depending on the orientation of the AGN disk plane and the mass and luminosity distance of the supermassive black hole. This is smaller than the statistical error here, but will need to be examined more carefully if a larger number of AGN-assisted binaries are used to measure  $H_0$ .

We computed the probability density of the Hubble constant using the distance probability density:

$$\begin{aligned} p(H_0|x_{\text{GW}}, d_L, \Omega_{\text{ZTF}}) &\propto \beta(H_0)^{-1} \int d d_L d \cos \iota \\ p(x_{\text{GW}}|d_L, \Omega_{\text{ZTF}}, z_{\text{ZTF}}) &\times p(H_0)p(d_L)p(\cos \iota), \end{aligned} \quad (3)$$

where  $\beta(H_0)$  is a normalization term that counts the expected number of detectable sources at given  $H_0$ ,  $x_{\text{GW}}$  is GW data,  $p(H_0)$  is the  $H_0$  prior, here we have considered uniform prior,  $p(d_L) \propto d_L^2$  is our distance prior, and  $p(\cos \iota)$  is our flat

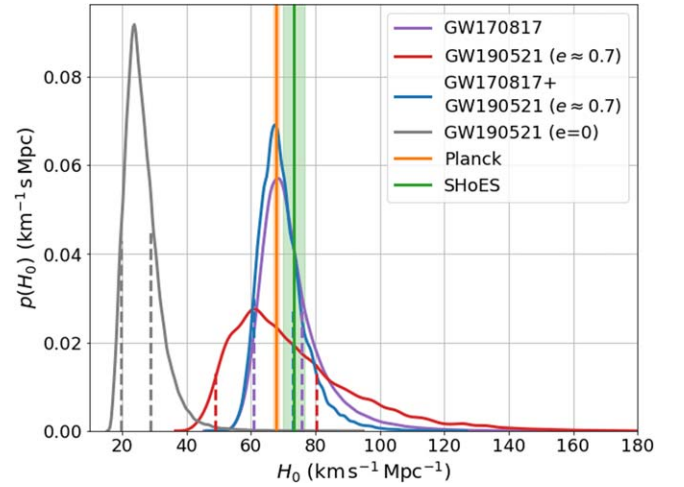


**Figure 3.**  $H_0$  measurements for GW190521 with its ZTF candidate counterpart and GW170817. The following  $H_0$  probability densities are shown: GW170817 (Abbott et al. 2017; purple); GW190521 with eccentric model (red); combined GW170817 and GW190521 with eccentric model (blue); GW190521 with  $e = 0$  (gray); cosmic microwave background results by Planck (orange); and Type Ia supernova results by ShoES (green). Shaded areas for the latter two results show 95% confidence intervals. Vertical dashed lines for the gravitational-wave results indicate 68% credible intervals.

inclination prior. Our priors are identical to those used by Abbott et al. (2017) to measure  $H_0$  using the binary neutron star merger GW170817.

For comparison, see Mukherjee et al. (2020) and Chen et al. (2020), who also computed  $p(H_0|\mathcal{D}_{\text{GW}}, \Omega_{\text{ZTF}}, z_{\text{ZTF}})$  for GW190521 for  $e = 0$ .

### 4. Results

Our  $H_0$  probability density from GW190521 based on the UF/RIT model (Gayathri et al. 2020b) and the ZTF candidate counterpart is shown in Figure 3. Numerically it is  $H_0 = 68.8_{-25.5}^{+45.7} \text{ km s}^{-1} \text{ Mpc}^{-1}$ . For comparison we show our  $H_0$  estimate for  $e = 0$ , which is  $H_0 = 25.4_{-7.9}^{+11.8} \text{ km s}^{-1} \text{ Mpc}^{-1}$ . We see that the distribution from the eccentric model has its maximum near the  $H_0$  values measured using Type Ia supernovae, which give a local expansion rate of  $H_0 = 74.03 \pm 1.42 \text{ km s}^{-1} \text{ Mpc}^{-1}$  (Riess et al. 2019), and the estimate from cosmic microwave background observations measured by the Planck Collaboration, which gives  $H_0 = 67.4 \pm 0.5 \text{ km s}^{-1} \text{ Mpc}^{-1}$  (Aghanim et al. 2018). The uncertainty is nevertheless significant. Our  $e = 0$  result is also consistent with the Type Ia/Planck  $H_0$  estimate.

We also show in Figure 3 the expected  $H_0$  estimate after combining the distributions obtained for GW190521 with that of GW170817. Here, we have used the marginalized posterior density for  $H_0$  from Abbott et al. (2017). We see that the improvement by this combination, as measured by the height of the probability density distribution, is a few percent, i.e., most information still comes from GW170817.

The above results assumed that the dark energy equation of state is  $w_0 = -1$ . Due to the relatively large distance of GW190521, this could lead to significant biases in our  $H_0$  estimate if this cosmology is incorrect (Shafieloo et al. 2020). We therefore estimated the cosmological parameters using a flat  $\Lambda$ CDM model, where we considered the flat priors on the cosmological parameters with ranges  $H_0 = [10, 200] \text{ km s}^{-1} \text{ Mpc}^{-1}$ ,  $\Omega_m = [0, 1]$ , and  $w_0 = [-2, -0.33]$ . We

obtain the cosmological parameters as  $H_0 = 104^{+36}_{-29}$   $\text{km s}^{-1}\text{Mpc}^{-1}$ ,  $\Omega_m = 0.46^{+0.35}_{-0.33}$ , and  $w_0 = -1.21^{+0.59}_{-0.54}$  for the eccentric case.

## 5. Conclusion





We estimated the Hubble constant using the luminosity distance of the gravitational-wave signal GW190521 and the redshift of its candidate electromagnetic counterpart detected by ZTF, assuming that the association is real. Identifying the host galaxy through electromagnetic radiation from a population of binary mergers may reduce the uncertainty of  $H_0$  reconstruction by an order of magnitude (Chen et al. 2018; Yang et al. 2020b; Del Pozzo 2012), making it potentially beneficial even if only a small fraction of black hole mergers produce detectable electromagnetic counterparts. For GW190521 we used the highly eccentric UF/RIT model (Gayathri et al. 2020b) with  $e \sim 0.7$ , and for comparison a noneccentric model similar to that of Abbott et al. (2020a). Our conclusions are as follows.

1. We find  $H_0 = 68.8^{+45.7}_{-25.5}$   $\text{km s}^{-1} \text{Mpc}^{-1}$  for GW190521 as a highly eccentric merger with  $e \sim 0.7$ .
2. Combining GW190521 and GW170817, we find  $H_0 = 68.5^{+15.9}_{-11.8}$   $\text{km s}^{-1} \text{Mpc}^{-1}$ .
3.  $H_0$  measurements using black hole mergers could be strongly affected if eccentricity is present and is not accounted for. For GW190521 we find a difference of  $\Delta H_0 \approx 60 \text{ km s}^{-1} \text{Mpc}^{-1}$  between the  $e \sim 0.7$  and  $e = 0$  cases we consider here.
4.  $H_0$  measurements using multiple AGN-assisted black hole mergers or mergers in galactic nuclei need to consider the effect of Doppler shift due to the binary's orbital velocity. In extreme cases, i.e., the mergers closest to the central supermassive black holes and orbital motion aligned with the line of sight, the systematic uncertainty in  $H_0$  due to the Doppler effect can be as large as 30%.

The authors are grateful to Will Farr for useful suggestions. The authors gratefully acknowledge the National Science Foundation (NSF) for financial support from grants No. PHY-1912632, No. PHY-1806165, No. PHY-1707946, No. ACI-1550436, No. AST-1516150, No. ACI-1516125, No. PHY-1726215, NSF AST-1516150, PHY-1707946, NASA TCAN grant No. 80NSSC18K1488, and the support of the Alfred P. Sloan Foundation. This work used the Extreme Science and Engineering Discovery Environment (XSEDE) [allocation TG-PHY060027N], which is supported by NSF grant No. ACI-1548562 and Frontera projects PHY-20010 and PHY-20007. Computational resources were also provided by the New-Horizons, BlueSky Clusters, and Green Prairies at the Rochester Institute of Technology, which were supported by NSF grants No. PHY-0722703, No. DMS-0820923, No. AST-1028087, No. PHY-1229173, and No. PHY-1726215. We are grateful for computational resources provided by the Leonard E Parker Center for Gravitation, Cosmology and Astrophysics at the University of Wisconsin-Milwaukee supported by NSF grant No. PHY-1626190. This research has made use of data, software, and/or web tools obtained from the Gravitational Wave Open Science Center (<https://www.gw-openscience.org>), a service of LIGO Laboratory, the LIGO Scientific Collaboration and the Virgo Collaboration. LIGO is funded by

the U.S. National Science Foundation. Virgo is funded by the French Centre National de Recherche Scientifique (CNRS), the Italian Istituto Nazionale della Fisica Nucleare (INFN), and the Dutch Nikhef, with contributions by Polish and Hungarian institutes.

## ORCID iDs

I. Bartos  <https://orcid.org/0000-0001-5607-3637>  
M. Campanelli  <https://orcid.org/0000-0002-8659-6591>  
C. O. Lousto  <https://orcid.org/0000-0002-6400-9640>  
R. O'Shaughnessy  <https://orcid.org/0000-0001-5832-8517>

## References

- Aasi, J., Abbott, B. P., Abbott, R., et al. 2015, *CQGr*, 32, 074001  
Abbott, B. P., Abbott, R., Abbott, T. D., et al. 2019, arXiv:1908.06060  
Abbott, B. P., Abbott, R., Abbott, T. D., et al. 2016, *PhRvD*, 94, 064035  
Abbott, B. P., Abbott, R., Abbott, T. D., et al. 2017, *Natur*, 551, 85  
Abbott, R., Abbott, T. D., Abraham, S., et al. 2020a, *PhRvL*, 125, 101102  
Abbott, R., Abbott, T. D., Abraham, S., et al. 2020b, *ApJL*, 900, L13  
Acernese, F., Agathos, M., Agatsuma, K., et al. 2015, *CQGr*, 32, 024001  
Aghanim, N., Akrami, Y., Ashdown, M., et al. 2018, arXiv:1807.06209  
Ashton, G., Ackley, K., Magaña Hernandez, I., & Piotrzkowski, B. 2020, arXiv:2009.12346  
Bartos, I., Haiman, Z., Marka, Z., et al. 2017a, *NatCo*, 8, 831  
Bartos, I., Kocsis, B., Haiman, Z., & Márka, S. 2017b, *ApJ*, 835, 165  
Belczynski, K. 2020, arXiv:2009.13526  
Calderón Bustillo, J., Sanchis-Gual, N., Torres-Forné, A., & Font, J. A. 2020, arXiv:2009.01066  
Chen, H.-Y., Fishbach, M., & Holz, D. E. 2018, *Natur*, 562, 545  
Chen, H.-Y., Haster, C.-J., Vitale, S., Farr, W. M., & Isi, M. 2020, arXiv:2009.14057  
Del Pozzo, W. 2012, *PhRvD*, 86, 043011  
Farrell, E. J., Groh, J. H., Hirschi, R., et al. 2020, arXiv:2009.06585  
Fragione, G., Loeb, A., & Rasio, F. A. 2020, *ApJL*, 902, L26  
Gayathri, V., Bartos, I., Haiman, Z., et al. 2020a, *ApJL*, 890, L20  
Gayathri, V., Healy, J., Lange, J., et al. 2020b, arXiv:2009.05461  
Giersz, M., Leigh, N., Hypki, A., Lützgendorf, N., & Askar, A. 2015, *MNRAS*, 454, 3150  
Graham, M. J., Ford, K. E. S., McKernan, B., et al. 2020, *PhRvL*, 124, 251102  
Hailey, C. J., Mori, K., Bauer, F. E., et al. 2018, *Natur*, 556, 70  
Healy, J., Lange, J., O'Shaughnessy, R., et al. 2018, *PhRvD*, 97, 064027  
Hogg, D. W. 1999, arXiv:astro-ph/9905116  
Lange, J., O'Shaughnessy, R., & Rizzo, M. 2018, arXiv:1805.10457  
Lange, J., O'Shaughnessy, R., Boyle, M., et al. 2017, *PhRvD*, 96, 104041  
LIGO and Virgo Scientific Collaborations 2019, GCN, 24621, 1  
McKernan, B., Ford, K. E. S., Bellovary, J., et al. 2018, *ApJ*, 866, 66  
Miller, M., & Hamilton, D. 2002, *MNRAS*, 330, 232  
Mukherjee, S., Ghosh, A., Graham, M. J., et al. 2020, arXiv:2009.14199  
O'Leary, R. M., Kocsis, B., & Loeb, A. 2009, *MNRAS*, 395, 2127  
O'Leary, R. M., Rasio, F. A., Fregeau, J. M., Ivanova, N., & O'Shaughnessy, R. 2006, *ApJ*, 637, 937  
Palmese, A., & Conselice, C. J. 2020, arXiv:2009.10688  
Riess, A. G., Casertano, S., Yuan, W., Macri, L. M., & Scolnic, D. 2019, *ApJ*, 876, 85  
Schutz, B. F. 1986, *Natur*, 323, 310  
Shafieloo, A., Keeley, R. E., & Linder, E. V. 2020, *JCAP*, 2020, 019  
Soares-Santos, M., Palmese, A., Hartley, W., et al. 2019, *ApJL*, 876, L7  
Stone, N. C., Metzger, B. D., & Haiman, Z. 2017, *MNRAS*, 464, 946  
Tagawa, H., Haiman, Z., Bartos, I., & Kocsis, B. 2020a, *ApJ*, 899, 26  
Tagawa, H., Haiman, Z., & Kocsis, B. 2020b, *ApJ*, 898, 25  
Varma, V., Field, S. E., Scheel, M. A., et al. 2019, *PhRvR*, 1, 033015  
Woosley, S. E., Blinnikov, S., & Heger, A. 2007, *Natur*, 450, 390  
Yang, Y., Bartos, I., Gayathri, V., et al. 2019b, *PhRvL*, 123, 181101  
Yang, Y., Bartos, I., Haiman, Z., et al. 2019a, *ApJ*, 876, 122  
Yang, Y., Bartos, I., Haiman, Z., et al. 2020, *ApJ*, 896, 138  
Yang, Y., Gayathri, V., Bartos, I., et al. 2020a, *ApJL*, 901, L34  
Yang, Y., Gayathri, V., Marka, S., Marka, Z., & Bartos, I. 2020b, arXiv:2009.13739